

ARTICLE OPEN



Arctic-associated increased fluctuations of midlatitude winter temperature in the 1.5° and 2.0° warmer world

Yungi Hong ¹, S.-Y. Simon Wang ², Seok-Woo Son ³, Jee-Hoon Jeong ⁴, Sang-Woo Kim ³, Baekmin Kim ⁵, Hyungjun Kim ⁶ and Jin-Ho Yoon ¹✉

In recent decades, the interior regions of Eurasia and North America have experienced several unprecedentedly cold winters despite the global surface air temperature increases. One possible explanation of these increasing extreme cold winters comes from the so-called Warm Arctic Cold Continent (WACC) pattern, reflecting the effects of the amplified Arctic warming in driving the circulation change over surrounding continents. This study analyzed reanalysis data and model experiments forced by different levels of anthropogenic forcing. It is found that WACC exists on synoptic scales in observations, model's historical and even future runs. In the future, the analysis suggests a continued presence of WACC but with a slightly weakened cold extreme due to the overall warming. Warm Arctic events under the warmer climate will be associated with not only a colder continent in East Asia but also a warmer continent, depending on the teleconnection process that is also complicated by the warmer Arctic. Such an increasingly association suggests a reduction in potential predictability of the midlatitude winter anomalies.

npj Climate and Atmospheric Science (2023)6:26; <https://doi.org/10.1038/s41612-023-00345-y>

INTRODUCTION

In recent decades, the Arctic region has warmed about twice as fast as the rest of the globe¹. Known as Arctic amplification (AA), this phenomenon is associated with the reduced sea ice and the increased surface air and ocean temperatures in the Arctic throughout the year^{2–4}. Meanwhile, extreme cold winters in the midlatitudes have become more frequent, hence creating the phenomenon known as the warm Arctic cold continent (WACC). The subject of WACC has attracted a lot of research attention as it provides a plausible explanation for the intensification of wintertime cold extremes⁵.

In the WACC framework, a fast decline of sea ice and an increase in winter SST in the Barents-Kara (BK) Sea is significantly correlated with a colder-than-usual winter climate in Eurasia. In contrast, a warmer east Siberian-Chukchi (ESC) Sea with less sea ice coverage is associated with abnormally cold winters in North America⁶. Various dynamical pathways have been proposed to explain these connections embedded in the intraseasonal time scales, including the weakening of the stratospheric polar vortex⁷, rapid Arctic tropospheric warming⁸, triggering of mid-tropospheric planetary waves along the midlatitudes and enhanced blocking in Ural regions^{9–11}. All these dynamical pathways are thought to have caused the midlatitude winter climate to become more extreme^{12,13}. Recent studies suggested that the formation of WACC is complex and difficult to attribute, since a wavier pattern of the jet can be entirely caused by the atmospheric internal variability, undermining the effect of AA^{14–20}. Despite the ongoing debate, a better understanding of WACC can improve the seasonal prediction of high-latitude climate, considering the importance of this mode in shaping weather and climate extremes in these regions.

This paper builds on the observed linkage between the Arctic and mid-latitude regions on synoptic scales over the past decades. It explores its historical and projected changes under current and 1.5-

and 2.0-degrees warming scenarios as determined by the Paris Agreement as the critical threshold to limit the strength of global warming. We analyze the Half degree additional warming, prognosis and projected impacts (HAPPI), a relatively new model projection dataset that has an advantage in assessing the impacts of 1.5- and 2.0-degrees warming on the world's weather²¹. Through this analysis, we assessed how WACC will vary through the synoptic linkage under different global warming scenarios, as well as identifying what the leading factor is in determining the dynamical changes.

RESULTS

Arctic-midlatitude relationships in observations

To establish the baseline for the association between the midlatitude and Arctic synoptic activities, we followed Kug et al. (2015) to examine the WACC patterns by conducting the regression analysis in two regions: BK Sea with East Asia and ESC Sea with North America. The regression coefficient between the BK (ESC) Sea and East Asia (North America) for each winter is shown as a time series in Fig. 1c, d. We also compute the geographical distribution of the average regression coefficients as regression maps (Fig. 1a, b): First, the winter-mean regression map is shown in the middle of Fig. 1 (1979~2018). Second, we display a few special winters: 1997/98 and 1991/92 were well-established warm Arctic and cold continent patterns, while 2017/18 and 2004/05 represent the warm Arctic and warm continent patterns.

Next, we examine the daily/synoptic weather fluctuation and how their supposed association may change over a longer period and in the future. In East Asia, most years show the negative regression coefficient of 850hPa temperature anomalies concerning the BK Sea (Fig. 1a, c). North America features a negative regression coefficient for the ESC Sea in most years (Fig. 1b, d). The negative regression coefficients between the Arctic and the

¹School of Earth Sciences and Environmental Engineering, Gwangju Institute of Science and Technology, Gwangju, South Korea. ²Department of Plants, Soils, and Climate, Utah State University, Logan, UT, USA. ³School of Earth and Environmental Science, Seoul National University, Seoul, South Korea. ⁴Department of Oceanography, Chonnam National University, Gwangju, South Korea. ⁵Department of Environmental Atmospheric Sciences, Pukyong National University, Busan, South Korea. ⁶Moon Soul Graduate School of Future Strategy, Korea Advanced Institute of Science and Technology, Daejeon, South Korea. ✉email: yjinho@gist.ac.kr

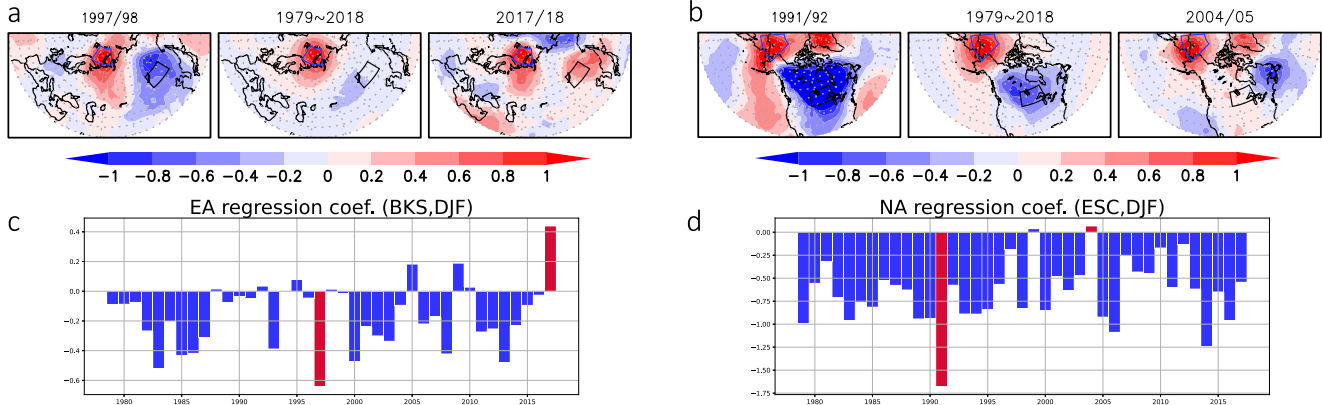


Fig. 1 Interannual variation of WACC. Regression coefficient of 850hPa temperature anomalies with respect to (a) the Barents-Kara sea (30° – 70° E, 70° – 80° N) and (b) East Siberia Chukchi sea (160° – 200° E, 65° – 80° N) 850hPa temperature anomalies during 1979/80–2017/18 winters from ERA-interim daily reanalysis data. Middle shows the regression coefficient from 1979 to 2018. Left and right shows the regression coefficient that is analyzed for 90 days when the regression coefficient is the smallest and biggest. **c, d** Time series of the regression coefficients of 850hPa temperature anomalies in East Asia (105° – 125° E, 47° – 55° N) and North America (255° – 275° E, 45° – 53° N) with respect to the Barents-Kara sea (30° – 70° E, 70° – 80° N) and East Siberia Chukchi sea (160° – 200° E, 65° – 80° N) 850hPa temperature anomaly during 1979/80–2017/18 winters (DJF), respectively. Black boxes indicate (a) the East Asia (105° – 125° E, 47° – 55° N) and (b) North America (255° – 275° E, 45° – 53° N). Blue boxes indicate (a) the Barents-Kara sea (30° – 70° E, 70° – 80° N) and (b) East Siberia Chukchi sea (160° – 200° E, 65° – 80° N).

midlatitude region have persisted during the past 40 years, suggesting that the WACC pattern is a steady climate oscillation in the intraseasonal/weather timescale (Fig. 1). However, we note that a few winters do not exhibit the typical pattern of WACC, like 2017/18 and 2004/05, suggesting a large interannual variation among this climatological feature.

Figure 1 confirms the previous observations that (1) the regression coefficients between the Arctic and mid-latitude temperatures in winter are mostly negative, and (2) the yearly regression coefficients do vary because some years can be noticeably positive, albeit not statistically significant. In other words, the winter temperature seesaw between the Arctic and the midlatitude regions is nonlinear and arguably unstable. Furthermore, past research has indicated that the climate linkage between the Arctic and midlatitude is not solely determined by their temperature contrast but also influenced by other factors such as sea surface temperature, reduction of sea ice, troposphere-stratosphere coupling, internal variability, and so on^{7,10,17,18,22–24}. Hence, projections of potential changes in the Arctic-midlatitude teleconnection under warmer climates remain uncertain.

Global warming impact on the relationship between the Arctic and midlatitude

Given the historical relationship between the temperature fluctuations in the Arctic and mid-latitude regions on the daily basis, we proceeded to analyze whether this relationship would persist in the future with global warming. In the HAPPI experiment Hist scenario, East Asia (North America) shows negative regression coefficients for the BK (ESC) Sea (Fig. 2a, b) and the peak of the regression coefficients in both East Asia and North America lies in the negative territory (Fig. 2c, d). The HAPPI experiment depicts the WACC pattern, which is shown in the reanalysis data, and it further reveals the WACC pattern in the Plus1.5 and Plus2.0 scenarios (even showing slightly stronger regression coefficients in East Asia compared to the Hist scenario; Supplementary Figs. 1 and 2). This result suggests that the WACC pattern persists under 1.5- and 2.0-degrees warming.

In all ensembles of the five models, the regression coefficient of each winter, a total of 4,500 winters, is displayed in a histogram (Fig. 2c, d). A histogram of the regression coefficients in East Asia shows that when 1.5- or 2.0-degrees warming occurs, the graph becomes more spread sideways compared to the Hist scenario

(Fig. 2c). The spread of the East Asia histogram in the Plus1.5 and Plus2.0 scenarios is due to the difference in temperature change in the BK Sea and East Asia. Although the average temperature increased overall due to global warming, the standard deviation of the temperature in the BK Sea decreased clearly (from 4.48 to 3.21 and 3.02) as global warming intensified (Fig. 2e). On the other hand, the standard deviation of the temperature in East Asia does not decrease clearly (from 5.51 to 5.45 and 5.40). Hence, the range of the East Asia regression coefficients explained by the BK Sea temperature increases in Plus1.5 and Plus2.0 scenarios (Fig. 2c), suggesting that the impact of the BK Sea on the temperature variation in East Asia increases. As a result, the consistency of Arctic-midlatitude teleconnection becomes weak.

Atmospheric circulations related to Arctic-midlatitude teleconnection

The increased temperature variation in East Asia appears to be related to the circulation change under Arctic warming. In the regression map of the geopotential height at 500hPa and surface pressure concerning the BK Sea near-surface temperature, there are positive pressure near the BK Sea and negative pressure in East Asia (Fig. 3). This high pressure near the BK Sea is a well-known circulation pattern related to WACC^{10,25}. Although the intensity of the low in East Asia does not change in the warming scenarios (Fig. 3a–c), the high over the BK Sea in Plus1.5 and Plus2.0 scenarios becomes more robust than in the Hist scenario (Fig. 3). Moreover, global warming enhances the 500hPa ridge over Eurasia, especially near the BK Sea rather than in other regions (Supplementary Fig. 3). These results suggest that the quasi-stationary high pressure over the BK Sea is linked to the enhanced Arctic-midlatitude teleconnection in the warmer climate, likely through a more substantial Rossby wave energy dispersion.

Sun et al. (2016) showed that the WACC would be weakened as the climate continues to warm²⁶. This is because the sea ice decline, SST variation, and radiative forcing in the Arctic are the key factors causing the warmer conditions over the midlatitude. Furthermore, in the CMIP5 simulations, the frequency of cold conditions over the midlatitude would decrease in the future²⁷. In other words, the WACC could be a transient phase of climate oscillation. However, based on our result, the co-variability of temperature between the Arctic and the midlatitude either remains the same or increases under the warmer climate.

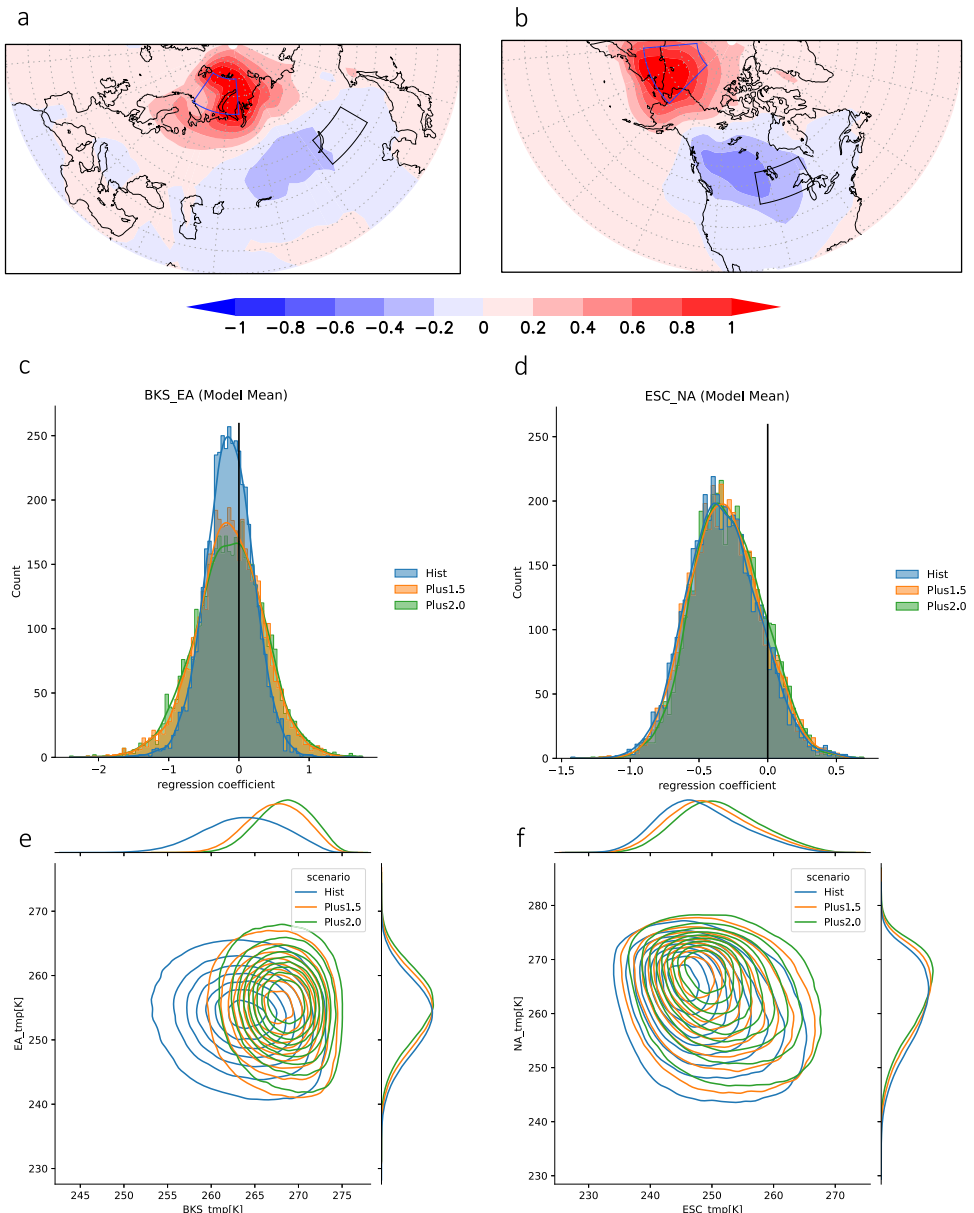


Fig. 2 Relationship between the Arctic and midlatitude under global warming. **a, b** The averaged regression coefficients of near-surface temperature with respect to the Barents-Kara sea (30° – 70° E, 70° – 80° N) and East Siberia Chukchi sea (160° – 200° E, 65° – 80° N) near-surface temperature from 5 models with 100-ensembles in HAPPI experiment Hist scenario. **c, d** The histogram of the regression coefficients in East Asia (105° – 125° E, 47° – 55° N) and North America (255° – 275° E, 45° – 53° N) with respect to the Barents-Kara sea and East Siberia Chukchi sea under HAPPI experiments Hist, Plus1.5 and Plus2.0 scenarios. **e, f** Joint plot of the temperature in East Asia and Barents-Kara, and North America and East Siberia Chukchi sea. Line in the box shows the kernel density estimation of the temperature. Top and right graph shows the distribution of the temperature. Hist, Plus1.5 and Plus2.0 scenario are represented in blue, orange and green respectively.

Moreover, 500hPa geopotential height composites show no significant changes in geopotential height over both the BK and East Asia in 1.5°C and 2.0°C warming compared to hist simulations (Supplementary Fig. 4a compared to c and e; b compared to d and f). These results indicate that colder-than-normal conditions over the midlatitude continent can still happen even under anomalous Arctic warming. In other words, the Arctic-midlatitude teleconnection will persist in the warmer climate even if the earth warms up by 2.0 degrees.

Process of the Arctic-midlatitude teleconnection

The causality between the Arctic and midlatitude is complex¹⁹, and the causes and effects of the WACC have not yet been

explicitly explained. To examine the causality between the BK Sea and East Asia, we adopt the granger causality method using daily winter temperature in the BK Sea and East Asia. We analyze 39 winters from ERA-interim and 4,500 winters (900 winters \times 5 models) from HAPPI experiments. There are more years in which the BK Sea temperature causes East Asia temperature than vice versa in the Granger causality test (Table 1). This can be further interpreted as East Asia temperature responds to the BK Sea temperature more frequently than the other way around, implying that the Arctic also has the potential to drive the midlatitude temperature anomalies. Even so, the co-existence of the Granger causality in both directions indicates complexity and uncertainty in the Arctic-midlatitude teleconnection.

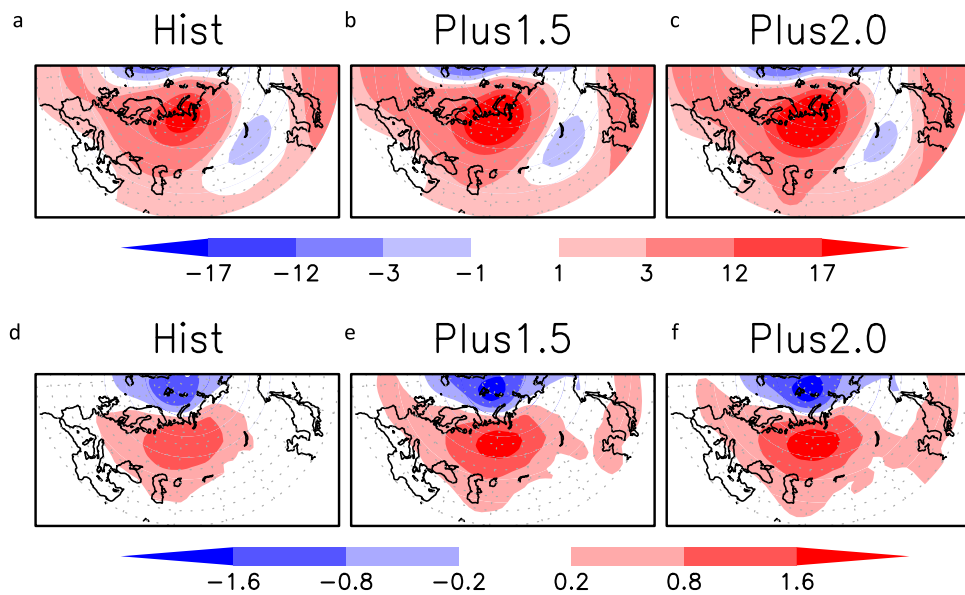


Fig. 3 The regression coefficient of pressure under different scenarios. **a–c** The averaged regression coefficients of geopotential height at 500hPa with respect to the Barents-Kara sea (30° – 70° E, 70° – 80° N) near-surface temperature from 5 models with 100-ensembles in HAPPI experiment Hist, Plus1.5 and Plus2.0 scenarios. **d–f** The averaged regression coefficients of surface pressure with respect to the Barents-Kara sea near-surface temperature from 5 models with 100-ensembles in HAPPI experiment Hist, Plus1.5 and Plus2.0 scenarios.

Table 1. The granger causality results between the Barents-Kara Sea (BKS) temperature and East Asia (EA) temperature in ERA-interim and HAPPI experiment.

Granger causality	ERA-interim	HAPPI experiment		
		Hist	Plus1.5	Plus2.0
BKS→EA	23	2041	1928	1847
EA→BKS	13	1454	1447	1408

39 winters from 1979 to 2018 are analyzed from ERA interim and 4,500 winters (900 winters \times 5 models) are analyzed from HAPPI experiment. Each number indicates the number of the year that shows a significant ($p \leq 0.05$) granger cause.

In the Granger causality analysis, we only used area-averaged surface air temperature. Hence, stratospheric pathways are not considered. Based on the Granger causality (Table 1) and the composite of 500hPa geopotential height anomaly (Supplementary Fig. 4) results, we produce the diagram (Fig. 4) to depict the possible path(s) of Arctic-midlatitude teleconnection. Using surface air temperature, one can see that there are more years in which BKS temperature leads to EA temperature than vice versa in reanalysis data and all scenarios in the HAPPI experiments. Moreover, high pressure at 500hPa over BKS is represented in both WACC and Warm Arctic Warm Continent (WAWC) conditions (Supplementary Fig. 4) while low pressure and high pressure at 500hPa over EA are represented depending on the WACC and WAWC, respectively. It suggests that the pressure patterns that appeared at WACC and WAWC are one of the mechanisms by which BKS temperature leads to EA temperature. Furthermore, as global temperature increases 1.5- or 2.0-degrees, the BK Sea warming and high pressure over the BK Sea would enhance (Figs. 2e, 3). The enhanced warming and geopotential height over the BK Sea would then cause a wilder temperature variance as the response to Arctic temperature fluctuations (Fig. 2c).

However, the limitation does exist in this explanation of the WACC teleconnection. First, there are bidirectional causes and effects between the high pressure over BKS and EA temperature

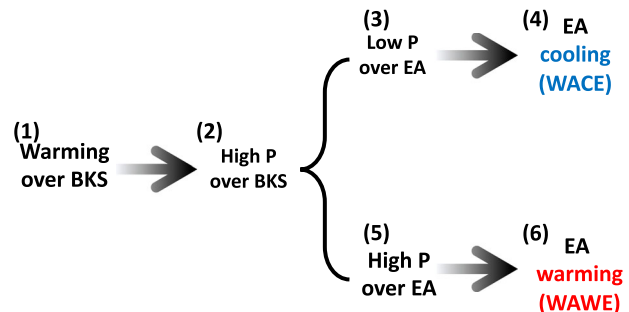


Fig. 4 Causality flow chart of the Arctic-midlatitude teleconnection. Flow of the Arctic-midlatitude teleconnection that explains cold and warm continent patterns under Arctic warming.

making it hard to determine the forcing from the response. Second, there are various climate factors that could cause Arctic warming and midlatitude cold¹⁹. An anomalous high pressure over BKS could be caused by other factors such as sea ice loss and internal variability. Additionally, Arctic upper tropospheric warming and associated troposphere-stratosphere coupling could trigger the Arctic-midlatitude teleconnection as well^{17,28}. Third, the mechanism of the circulation interlink between BKS and EA is not well reproduced by models. To explicitly understand the teleconnection between the Arctic and mid-latitude, a further study that provides knowledge about the dynamic processes causing the WACC pattern is needed. For example, the dynamical processes can be further diagnosed with detailed budget analyses of heat, vorticity, and geopotential tendency of multiple layers from both reanalysis (such as Kim et al. 2021)²⁹ and sensitivity experiments that prescribe sea ice loss such as those associated with Polar Amplification Model Intercomparison Project (PAMIP).

DISCUSSION

This study identifies whether the association between the daily Arctic and midlatitude temperature fluctuations would change under the warmer climate targeted by the 2015 Paris Agreement. We used the HAPPI experiments to investigate the change in this

Arctic-midlatitude teleconnection. First, it is found that a somewhat steady negative regression between the Arctic and mid-latitude temperatures supports the recent trend in Arctic warming and midlatitude cooling. However, in the HAPPI experiment, the range of East Asia's temperature regression coefficient increases under both the 1.5- and 2.0-degree warming scenarios. Such a fluctuation in the teleconnection may be associated with the faster warming in the BK Sea associated with a reduced standard deviation of temperature. The increased range of regression coefficients indicates that temperature variation in East Asia could increase but its correspondence with Arctic warming would become less stable. This result echoes Jung (2020)'s finding that global warming could decrease the forecast skills of Arctic-midlatitude teleconnection³⁰.

Most earlier studies debating the WACC and AA relationship focused on the trend or decadal change. This study explores the specific warming levels and associated change of the midlatitude temperature fluctuation related to Arctic warming in the synoptic timescale. However, this study does not attempt to challenge whether the AA or sea ice loss is a trigger of the frigid winters. We also recognize that tropical forcing, the main source of internal variability in the midlatitudes, particularly sea surface temperature changes in the East Pacific³¹, can also cause the WACC pattern^{16,18}. The disparity of the WACC responses between the observation and model simulations remains the critical factor that complicates the diagnostics⁵ and requires continued research on the various interactions between the Arctic and midlatitude weather.

Global warming increases the tropospheric geopotential height overall, but the increased highs in the BK Sea and East Asia are also attributable to the warm continent patterns. Meanwhile, the positive and negative circulation, called dipole patterns and related to cold continent patterns³², still exist in the 1.5- and 2-degree Celsius warming scenarios. The duration and frequency of the extreme cold do not change significantly in global warming scenarios, despite a weakened trend in the intensity of cold events³³. Hence, the persistent existence of circulation patterns related to WACC under warming scenarios provides the possibility that the Arctic-midlatitude teleconnection is very likely to remain in the future with global warming. Moreover, the increased fluctuation in the response of East Asia temperature to Arctic temperature under global warming makes the mechanism of the Arctic-midlatitude teleconnection more complicated and its prediction difficult.

METHODS

Data

It was reported that Arctic tropospheric warming has caused cooling trends in the midlatitudes through increasing the southward propagating Rossby wave train and impacting the intensity of the Siberian High^{28,34}. Given that the Siberian High is a lower-tropospheric feature, we used the 850hPa daily temperature from the European Center for Medium-Range Weather Forecasting (ECMWF) reanalysis (ERA-interim) with a spatial resolution of $1^\circ \times 1^\circ$ from 1979 to 2018³⁵ in our study. First, leap days are excluded from all daily temperature reanalysis data. Then, daily anomalies are calculated by subtracting the climatology from each daily value from 1979 to 2018.

The HAPPI experiment is used for analyzing the impact of global warming on the relationship between the Arctic and midlatitude. A total of 5 models (CAM4, CanAM4, ECHAM6, NorESM1, MIROC5) with 100 ensembles each are used with three scenarios: Hist, i.e., the current decade (2006–2015), 1.5- (Plus 1.5) and 2.0- (Plus 2.0) degrees warming scenarios, respectively. The HAPPI models do not provide consistent outputs. We selected models with all three experiments (Hist, Plus1.5, and Plus2.0 scenarios) with the largest number of ensemble members. Each ensemble of the scenarios

contains ten years. In other words, a total of 1000 years of daily data for each model is analyzed. In the CMIP experiment, the uncertainty of global warming impact increases with time since it is based on the emission scenario approach. On the other hand, the HAPPI experiment simulates the effect of global warming at specified goals, such as 1.5- and 2.0-degrees, by constraining global temperature with large ensemble members²¹. In this regard, HAPPI is more suitable for identifying regional responses and extreme weather events caused by 1.5- and 2.0-degrees warming than other coupled model simulations. The 1.5- and 2.0-degrees warming scenarios are generated using forcing values for anthropogenic factors from RCP2.6 and RCP4.5 experiments in 2095.

Regression analysis

Regression analysis is applied to evaluate the changing inter-annual links between the Arctic and midlatitudes. In ERA-interim daily data, a regression analysis is performed for 90 days of each winter from 1979 to 2018 by dividing the regions: East Asia (explained by the BK Sea) and North America (explained by the ESC Sea). The HAPPI experiment uses the daily near-surface temperature of five models in Hist, Plus1.5, and Plus2.0 scenarios. Since each ensemble has nine winters, regression analysis is conducted for 810 days in winter per ensemble. Then, the ensemble mean of the regression coefficient is calculated for each model. Moreover, to identify the distribution of the regression coefficient for each winter, 4,500 regression coefficients (900 regression coefficients \times 5 models) in winter are calculated and displayed as a histogram. Finally, these steps are equally applied to Hist, Plus1.5, and Plus2.0 scenarios.

Granger Causality

Granger causality is an approach to diagnosing the causality between two variables originally suggested by Clive E. Granger³⁶. Granger causality determines whether one variable helps predict another variable statistically. In the case of climate variables, this could imply causality more appropriately when one or more variables have a longer memory than traditional lagged regression analysis³⁷. It simply consists of a lagged autocorrelation and a lagged multiple linear regression.

$$X_t = a_0 + a_1 X_{t-1} + a_2 X_{t-2} + \cdots + a_k X_{t-k} + d_t \quad (1)$$

$$X_t = c_0 + c_1 Y_{t-1} + c_2 Y_{t-2} + \cdots + c_k Y_{t-k} + (b_1 Y_{t-1} + b_2 Y_{t-2} + \cdots + b_k Y_{t-k}) + d_t \quad (2)$$

Equation (1) is the autocorrelation of X_t with lag k and Eq. (2) is multiple linear regression using X_t and Y_t with lag k. In this study, X_{t-k} indicates k days lagged variable and d_t is error term. If multiple linear lagged regression (Eq. (2)) explains significantly more variance in X than autoregression (Eq. (1)), it is said that Y granger-causes X . There are two steps to assess significance. First, at least one value of b should be significant according to a two-sided t test. Second, the square of the difference between Eqs. (1) and (2) should be significant according to an F-test. In this study, the Granger model is conducted iteratively through each daily sequence by defining the k, sequence from 1 day to 18 days. Then, we counted the year which shows a significant difference between Eqs. (1) and (2). X and Y are temperature in the BK Sea and East Asia. We perform the regression analysis in both directions, $X \rightarrow Y$ and $Y \rightarrow X$.

DATA AVAILABILITY

The meteorological data is retrieved from the ERA-interim by the European Center for Medium-Range Weather Forecast (ECMWF) at <http://www.ecmwf.int/en/forecasts/datasets/reanalysis-datasets/era-interim/>. The HAPPI data can be accessed from <https://portal.nersc.gov/c20c/data.html>. Derived data supporting the findings of this study are available from the corresponding author upon reasonable request.

CODE AVAILABILITY

The source codes for the analysis of this study are available from the corresponding author upon reasonable request.

Received: 26 August 2022; Accepted: 9 March 2023;

Published online: 27 March 2023

REFERENCES

1. Stocker, T. F. et al. Climate change 2013 the physical science basis: Working Group I contribution to the fifth assessment report of the intergovernmental panel on climate change. *Clim. Chang. 2013 Phys. Sci. Basis Work. Gr. I Contrib. Fifth Assess. Rep. Intergov. Panel Clim. Chang.* **9781107057**, 1–1535 (2013).
2. Screen, J. A. & Simmonds, I. The central role of diminishing sea ice in recent Arctic temperature amplification. *Nature* **464**, 1334–1337 (2010).
3. Stroeve, J., Holland, M. M., Meier, W., Scambos, T. & Serreze, M. Arctic sea ice decline: Faster than forecast. *Geophys. Res. Lett.* **34**, L09501 (2007).
4. Kim, K. Y. et al. Vertical Feedback Mechanism of Winter Arctic Amplification and Sea Ice Loss. *Sci. Rep.-Uk* **9**, 1184 (2019).
5. Cohen, J. et al. Divergent consensuses on Arctic amplification influence on midlatitude severe winter weather. *Nat. Clim. Change* **10**, 20–29 (2020).
6. Kug, J. S. et al. Two distinct influences of Arctic warming on cold winters over North America and East Asia. *Nat. Geosci.* **8**, 759–762 (2015).
7. Kim, B. M. et al. Weakening of the stratospheric polar vortex by Arctic sea-ice loss. *Nat. Commun.* **5**, 4646 (2014).
8. Wang, S. Y. S. et al. Accelerated increase in the Arctic tropospheric warming events surpassing stratospheric warming events during winter. *Geophys. Res. Lett.* **44**, 3806–3815 (2017).
9. Luo, B. H. & Yao, Y. Recent Rapid Decline of the Arctic Winter Sea Ice in the Barents-Kara Seas Owing to Combined Effects of the Ural Blocking and SST. *J. Meteorol. Res.-Prc.* **32**, 191–202 (2018).
10. Luo, D. H. et al. Impact of Ural Blocking on Winter Warm Arctic-Cold Eurasian Anomalies. Part I: Blocking-Induced Amplification. *J. Clim.* **29**, 3925–3947 (2016).
11. Semenov, V. A. & Latif, M. Nonlinear winter atmospheric circulation response to Arctic sea ice concentration anomalies for different periods during 1966–2012. *Environ. Res. Lett.* **10**, 054020 (2015).
12. Chien, Y. T. et al. North American Winter Dipole: Observed and Simulated Changes in Circulations. *Atmosphere-Basel* **10**, 793 (2019).
13. Cohen, J. et al. Recent Arctic amplification and extreme mid-latitude weather. *Nat. Geosci.* **7**, 627–637 (2014).
14. Blackport, R. & Screen, J. A. Insignificant effect of Arctic amplification on the amplitude of midlatitude atmospheric waves. *Sci. Adv.* **6**, eaay2880 (2020).
15. Blackport, R., Screen, J. A., van der Wiel, K. & Bintanja, R. Minimal influence of reduced Arctic sea ice on coincident cold winters in mid-latitudes. *Nat. Clim. Change* **9**, 697–704 (2019).
16. Collow, T. W., Wang, W. Q. & Kumar, A. Simulations of Eurasian winter temperature trends in coupled and uncoupled CFSv2. *Adv. Atmos. Sci.* **35**, 14–26 (2018).
17. Francis, J. A. Why Are Arctic Linkages to Extreme Weather Still up in the Air? *Bull. Am. Meteorol. Soc.* **98**, 2551–2557 (2017).
18. McCusker, K. E., Fyfe, J. C. & Sigmond, M. Twenty-five winters of unexpected Eurasian cooling unlikely due to Arctic sea-ice loss. *Nat. Geosci.* **9**, 838–842 (2016).
19. Overland, J. E. et al. Nonlinear response of mid-latitude weather to the changing Arctic. *Nat. Clim. Change* **6**, 992–999 (2016).
20. Sorokina, S. A., Li, C., Wettstein, J. J. & Kvamstø, N. G. Observed Atmospheric Coupling between Barents Sea Ice and the Warm-Arctic Cold-Siberian Anomaly Pattern. *J. Clim.* **29**, 495–511 (2016).
21. Mitchell, D. et al. Half a degree additional warming, prognosis and projected impacts (HAPPI): background and experimental design. *Geosci. Model Dev.* **10**, 571–583 (2017).
22. Li, M. et al. Anchoring of atmospheric teleconnection patterns by Arctic Sea ice loss and its link to winter cold anomalies in East Asia. *Int. J. Climatol.* **41**, 547–558 (2021).
23. Luo, X. & Wang, B. How predictable is the winter extremely cold days over temperate East Asia? *Clim. Dyn.* **48**, 2557–2568 (2016).
24. Tang, Q. H., Zhang, X. J., Yang, X. H. & Francis, J. A. Cold winter extremes in northern continents linked to Arctic sea ice loss. *Environ. Res. Lett.* **8**, 014036 (2013).
25. Overland, J. et al. The Melting Arctic and Midlatitude Weather Patterns: Are They Connected?*. *J. Clim.* **28**, 7917–7932 (2015).
26. Sun, L., Perlitz, J. & Hoerling, M. What caused the recent "Warm Arctic, Cold Continents" trend pattern in winter temperatures? *Geophys. Res. Lett.* **43**, 5345–5352 (2016).
27. Mori, M., Watanabe, M., Shiogama, H., Inoue, J. & Kimoto, M. Robust Arctic sea-ice influence on the frequent Eurasian cold winters in past decades. *Nat. Geosci.* **7**, 869–873 (2014).
28. He, S. P., Xu, X. P., Furevik, T. & Gao, Y. Q. Eurasian Cooling Linked to the Vertical Distribution of Arctic Warming. *Geophys. Res. Lett.* **47**, e2020GL087212 (2020).
29. Kim, H. J., Son, S. W., Moon, W., Kug, J. S. & Hwang, J. Subseasonal relationship between Arctic and Eurasian surface air temperature. *Sci. Rep.-Uk* **11**, 4081 (2021).
30. Jung, E. et al. Impacts of the Arctic-midlatitude teleconnection on wintertime seasonal climate forecasts. *Environ. Res. Lett.* **15**, 094045 (2020).
31. Feng, X. F. et al. A Multidecadal-Scale Tropically Driven Global Teleconnection over the Past Millennium and Its Recent Strengthening. *J. Clim.* **34**, 2549–2565 (2021).
32. Park, T. W., Ho, C. H. & Deng, Y. A synoptic and dynamical characterization of wave-train and blocking cold surge over East Asia. *Clim. Dyn.* **43**, 753–770 (2014).
33. Ayarzagüena, B. & Screen, J. A. Future Arctic sea ice loss reduces severity of cold air outbreaks in midlatitudes. *Geophys. Res. Lett.* **43**, 2801–2809 (2016).
34. Ye, K. H., Jung, T. & Semmler, T. The Influences of the Arctic Troposphere on the Midlatitude Climate Variability and the Recent Eurasian Cooling. *J. Geophys. Res.-Atmos.* **123**, 10143–10165 (2018).
35. Dee, D. P. et al. The ERA-Interim reanalysis: configuration and performance of the data assimilation system. *Q. J. R. Meteorol. Soc.* **137**, 553–597 (2011).
36. Granger, C. W. J. Investigating Causal Relations by Econometric Models and Cross-spectral Methods. *Econometrica* **37**, 424 (1969).
37. McGraw, M. C. & Barnes, E. A. Memory Matters: A Case for Granger Causality in Climate Variability Studies. *J. Clim.* **31**, 3289–3300 (2018).

ACKNOWLEDGEMENTS

This was supported by the GIST research institute funded by the GIST in 2023 and the National Research Foundation of Korea under NRF-2021R1A2C1011827 and NRF-2020M1A5A1110578. S.-Y. Wang was supported by the U.S. Department of Energy, Office of Science, under Award number DE-SC0016605 and by the U.S. SERDP program under RC20-3056.

AUTHOR CONTRIBUTIONS

Y.H.: Investigation, Visualization, Analysis, Writing-Original draft, Reviewing, Editing. S.-Y. (Simon) W.: Conceptualization, Writing, Reviewing, Editing, Supervision. S.-W.S.: Methodology, Writing, Reviewing, Editing. J.-H.J.: Writing, Reviewing, Editing. S.-W.K.: Writing, Reviewing, Editing. B.K.: Writing, Reviewing, Editing. H.K.: Data, Writing, Reviewing, Editing. J.-H.Y.: Conceptualization, Investigation, Writing, Reviewing, Editing, Supervision.

COMPETING INTERESTS

The authors declare no competing interests.

ADDITIONAL INFORMATION

Supplementary information The online version contains supplementary material available at <https://doi.org/10.1038/s41612-023-00345-y>.

Correspondence and requests for materials should be addressed to Jin-Ho Yoon.

Reprints and permission information is available at <http://www.nature.com/reprints>

Publisher's note Springer Nature remains neutral with regard to jurisdictional claims in published maps and institutional affiliations.



Open Access This article is licensed under a Creative Commons Attribution 4.0 International License, which permits use, sharing, adaptation, distribution and reproduction in any medium or format, as long as you give appropriate credit to the original author(s) and the source, provide a link to the Creative Commons license, and indicate if changes were made. The images or other third party material in this article are included in the article's Creative Commons license, unless indicated otherwise in a credit line to the material. If material is not included in the article's Creative Commons license and your intended use is not permitted by statutory regulation or exceeds the permitted use, you will need to obtain permission directly from the copyright holder. To view a copy of this license, visit <http://creativecommons.org/licenses/by/4.0/>.

© The Author(s) 2023